



Calculation of left ventricular ejection fraction using an 8-layer residual U-Net with deep supervision based on cardiac CT angiography images versus echocardiography: a comparative study

Jingyuan Zhang¹, Lin Yang², Yumeng Hu³, Xiaochang Leng³, Wenhao Huang¹, Yajun Liu¹, Xiaowei Liu¹, Lin Wang¹, Jianjun Zhang⁴, Danyun Li⁴, Lijiang Tang¹, Jianping Xiang³, Changqing Du¹

¹Department of Cardiology, Zhejiang Hospital, Hangzhou, China; ²Department of Geriatrics, The First Affiliated Hospital, Zhejiang University School of Medicine, Hangzhou, China; ³ArteryFlow Technology Co., Ltd., Hangzhou, China; ⁴Department of Radiology, Zhejiang Hospital, Hangzhou, China

Contributions: (I) Conception and design: All authors; (II) Administrative support: C Du; (III) Provision of study materials or patients: C Du, X Leng, J Xiang, L Tang; (IV) Collection and assembly of data: All authors; (V) Data analysis and interpretation: Jingyuan Zhang, C Du, Y Hu; (VI) Manuscript writing: All authors; (VII) Final approval of manuscript: All authors.

Correspondence to: Changqing Du, MD. Department of Cardiology, Zhejiang Hospital, 1229 Gudun Road, Xihu District, Hangzhou 310013, China. Email: ddcq82@126.com.

Background: Accurate segmentation of the left ventricle (LV) is an important step in assessing cardiac function. Cardiac CT angiography (CCTA) has become an important means of clinical diagnosis of cardiovascular diseases (CVDs) because of its advantages of non-invasive, short examination time and low cost. In order to obtain the segmentation of LV in CCTA scans, we propose a deep learning method based on 8-layer residual U-Net with deep supervision. In this study we compared the left ventricular ejection fraction (LVEF) calculated by deep learning (DL) method (AccuLV) from CCTA to LVEF by conventional two-dimensional echocardiography (EC).

Methods: This was a retrospective cross-sectional study, and consecutive patients who had undergone CCTA and EC in our hospital from February 2021 to May 2021 were recruited. The current study included 180 patients who had undergone CCTA and EC. To obtain LVEF, we used an 8-layer residual U-Net with deep supervision to segment LV contours from CCTA images and compute LVEF (DL-LVEF). The EC and DL-LVEF measurements were compared. A 50% EC-LVEF cut-off value was used as a reference standard to assess the diagnostic performance of AccuLV in assessing LV function.

Results: The overall mean EC-LVEF and DL-LVEF values were 64.0% (52.3%, 69.0%) and 73.0% (52.3%, 77.0%), respectively. Three patient groups were studied: (I) hypertensive patients, (II) postmenopausal women, and (III) diabetes. EC-LVEF and DL-LVEF were found to be positively correlated for all of the included patients ($r=0.82$, $P<0.001$), with the detailed results for the three groups as follows: hypertensive patients ($r=0.77$, $P<0.001$), postmenopausal women ($r=0.92$, $P<0.001$) and diabetes ($r=0.88$, $P<0.001$). The diagnostic accuracy, sensitivity, and specificity of the DL method in predicting EC-LVEF $<50\%$ for all patients were 93.9%, 92.3%, and 94.3%, and for hypertensive patients were 95.4%, 93.8%, and 95.8%, for postmenopausal women were 87.0%, 100%, and 84.2%, for diabetes were 97.4%, 100%, and 96.6%.

Conclusions: In comparison to echocardiography, which is commonly used in clinical setting, AccuLV may be a promising, fully automated tool for rapid and accurate quantification of LV function and thus for making reliable clinical decisions.

Keywords: Deep learning (DL); U-Net; segmentation; left ventricle; computed tomography; echocardiography (EC)

Submitted Sep 17, 2022. Accepted for publication Jul 28, 2023. Published online Aug 15, 2023.

doi: 10.21037/qims-22-976

View this article at: <https://dx.doi.org/10.21037/qims-22-976>

Introduction

Cardiovascular disease (CVD) currently stands as the foremost cause of mortality worldwide (1). The left ventricular ejection fraction (LVEF) serves as a significant prognostic indicator for CVD, encompassing heart failure (2), acute myocardial infarction (3), and valvular heart disease (4). The indications of certain medical conditions rely on the LVEF values (5). Moreover, objective evaluations of LVEF aid in the classification and determination of treatment approaches for heart failure (6). LVEF measurements also play a pivotal role in decision-making processes regarding coronary artery bypass grafting and heart valve surgeries (7,8). Consequently, precise quantification of left ventricular (LV) function is imperative.

LVEF can be assessed clinically by cardiac magnetic resonance, cardiac catheterization, and echocardiography (EC), of which EC is the most widely used due to its advantages of being noninvasive, low cost, and quick (9). Nevertheless, segmentation challenges are exacerbated by the presence of speckled noise in acquired images and irregular alterations in physiological structures attributable to individual variations among patients. Manual delineation of the LV is labor-intensive, influenced by subjective factors, and demands a high degree of technical proficiency from medical professionals. As a result, a fully automated, accurate, and rapid method for quantifying LV function is highly desirable.

In recent years, with the continuous development of deep learning (DL) algorithm, more and more researchers have applied DL algorithm to the evaluation of LV function (10). In the field of LV function recognition, there are many unsolved problems, such as difficulty in obtaining training samples, high difficulty in labeling and slow model reasoning.

To address the problems of the above methods, we propose an 8-layer residual U-Net method based on Cardiac CT angiography (CCTA) images for automatic segmentation of LV. U-Net is a u-shaped network based on fully convolutional network (FCN), where the skip connection is in the form of concatenation instead of summation to concatenate the shallow and deep feature maps for improving the utilization of feature channels and better restoring the

details (11). It does not require a large amount of training data and is suitable for medical image segmentation (11). Based on the original 4-layer U-Net, our method deepens the number of layers to 8 layers to extract deeper level of abstract information, and introduces an auxiliary path for deep supervision (12), so that losses can be obtained from the deep feature map and the segmentation accuracy of the model can be improved. The primary objective of this research is to verify the accuracy of the DL algorithm in assessing LV function, using EC as the reference standard. We present this article in accordance with the STARD reporting checklist (available at <https://qims.amegroups.com/article/view/10.21037/qims-22-976/rc>).

Methods

Patient enrollment

It was a single-center, retrospective study. Two hundred sixty-two patients were consecutively enrolled from February 2021 to May 2021. Patients who had undergone CCTA and two-dimensional EC within 7 days were eligible. Exclusion criteria included age <18 years, renal insufficiency (serum creatinine >1.5 mg/dL), and other common arrhythmias, acute myocardial infarction, age \geq 80 years old, and poor quality of CCTA images. Indications for CCTA included patients with confirmed or suspected coronary artery disease. Inclusion criteria for CCTA images were: layer thickness \leq 0.75 mm, adequate signal-to-noise ratio, no serious motion/metal artifact. The research was carried out in accordance with the Declaration of Helsinki (as revised in 2013). The study was approved by the Ethics Committee of Zhejiang Hospital. Since this clinical study was a retrospective analysis of the information of previous cases, without direct contact with the subjects, the risk borne by the subjects was not greater than the minimum risk. The Ethics Committee of Zhejiang Hospital agreed to exempt informed consent after review.

CT acquisition protocol and EC

A dual-source CT scanner was used for the CCTA (Siemens Healthineers, Erlangen, Germany). 50–70 mL contrast agent

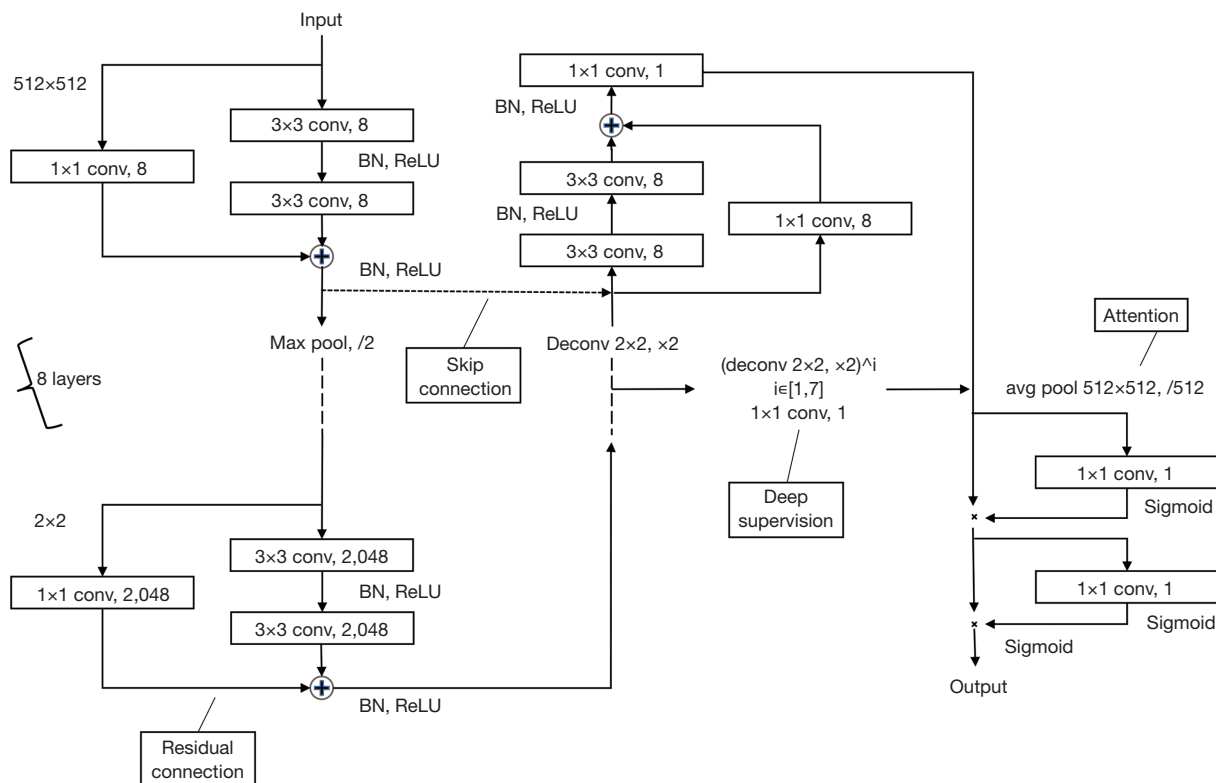


Figure 1 Model architecture of AccuLV software based on the deep neural network of U-Net for segmentation of the left ventricular myocardium from CCTA. BN, batch normalization; ReLU, rectified linear unit; AccuLV, left ventricular ejection fraction calculated by deep learning method; CCTA, coronary computed tomography angiography.

(Iopromide, 370 mgI/mL; Bayer, Leverkusen, Germany) was administered intravenously (4.5 mL/s injection speed), followed by rinsing with 40 mL saline. The CT scanning was performed using a retrospective electrocardiography-gating mode. Detailed scanning parameters were as follows: detector collimation (32×0.6 mm) combined with z-flying focal spot technology, gantry rotation time of 330 ms, tube voltage of 120 kVp, tube current of 400 mAs, and a craniocaudal scan direction.

The patients were scanned in left-lateral decubitus using an iE33 ultrasound system (Philips Medical Systems, Andover, MA, USA) for EC, with images obtained in standard apical and parasternal views. The papillary muscle in the LV cavity was included after manually tracing the endocardium profile on two- and four-chamber views of end-diastole and end-systole. And the Simpson biplane method was used to calculate the LVEF. LVEF was calculated using end-diastole and end-systole volumes and LVEF <50% was considered abnormal (13).

DL-LVEF computation

DL-LVEF was computed using a dedicated software (AccuLV, version 1.0, ArteryFlow Technology Co., Ltd., Hangzhou, China). Its model architecture was based on the deep neural network of U-Net, as previously described (12), as shown in *Figure 1*. It was made up of 8 layers that were included in both the contracting and expanding paths. Each layer included two sets of convolution with a kernel of 3×3 pixels, batch normalization (BN), and rectified linear unit (ReLU) activation. Each layer was built with a residual connection. The output of the second 3×3 convolution was added to the input to each layer via a 1×1 convolution. Using max pooling, the output from each layer in the contracting path was down-sampled to reduce the resolution by half. The input from each layer in the expanding path was up-sampled to recover resolution using deconvolution with a kernel of 2×2 pixels and a stride of 2 pixels, and was then concatenated with the output from

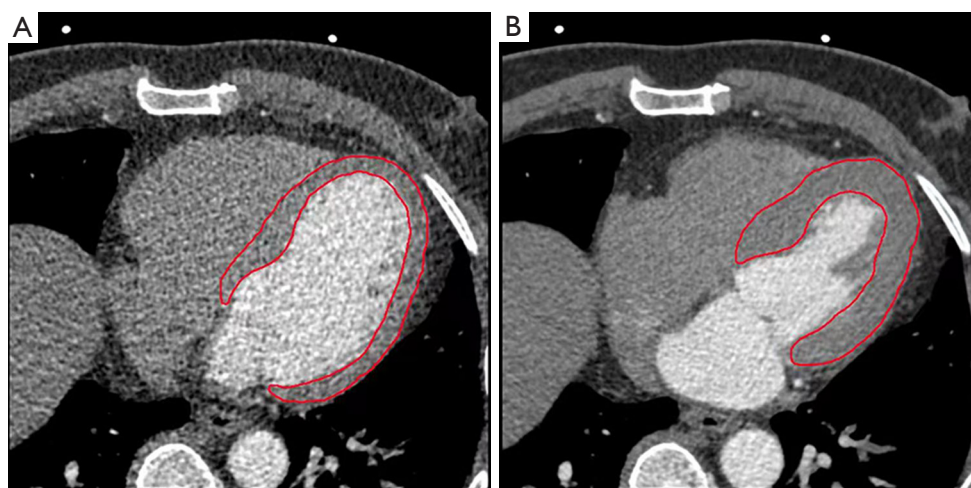


Figure 2 A case of calculation of left ventricular ejection fraction. (A) The left ventricular segmentation at end-diastole to calculate EDV, and (B) the left ventricular segmentation at end-systole to calculate ESV, the $SV = EDV - ESV$ and the ejection fraction $EF = SV/EDV$. EDV, end-diastolic volume; ESV, end-systolic volume; SV, stroke volume.

the corresponding layer in the contracting path using skip connection in the form of concatenation. In the contracting path, the first layer's input channel was increased from 1 to 8 and the others were doubled. The input channel at each layer was halved in the expanding path, the output channel at the final layer was reduced from 8 to 1 using a 1×1 convolution, and the branch from here served as the main output branch.

As deep supervision, seven auxiliary output branches were added before the first seven layers of the expanding path. To recover the same resolution as the main output branch, each branch consisted of 1 to 7 consecutive 2×2 deconvolutions and a 1×1 convolution. Following the 7 auxiliary output branches and the main output branch, the attention was added. The global down-sampling was performed using average pooling, followed by a set of a 1×1 convolution and a sigmoid activation to obtain the weight of the current branch. To increase the focus on the key branches, feature maps from different branches were multiplied by different weights. To obtain the spatial weights of the current branch, a set of a 1×1 convolution and a sigmoid activation was added again. To draw attention to key regions, feature maps from various spatial locations were multiplied by different weights. Finally, the feature maps were subjected to sigmoid activation to obtain pixel-wise probabilities of belonging to the foreground (>0.5) or background (≤ 0.5). After the

segmentation of LV with the U-Net model, LVEF can be then computed. The computation of LVEF involves dividing the stroke volume by the end-diastolic volume (EDV). Representative example is shown in *Figure 2*.

Statistical analysis

SPSS 20.0 (IBM Corp., Armonk, NY, USA) and MedCalc 19.0.4 (MedCalc Software Inc., Ostend, Belgium) software were used for statistical analysis. To test the normality of continuous variables, the Kolmogorov-Smirnov method was used. Continuous variables with a normal distribution were recorded as mean \pm SD, while continuous variables with a skewed distribution were expressed as median [interquartile range (IQR)]. Categorical variables are denoted by the letter n (%). Using the European and American guidelines for heart failure as a guideline, LVEF $\geq 50\%$ indicates normal LV systolic function. The accuracy, specificity, sensitivity, positive predictive value (PPV), negative predictive value (NPV), and area under the curve (AUC) of the DL method in judging LVEF were determined using EC as the reference standard. To calculate the limits of agreement for LVEF, a Bland-Altman analysis was performed. The Pearson correlation coefficient was used to examine the relationship between them. $P < 0.05$ was considered as statistically significant.

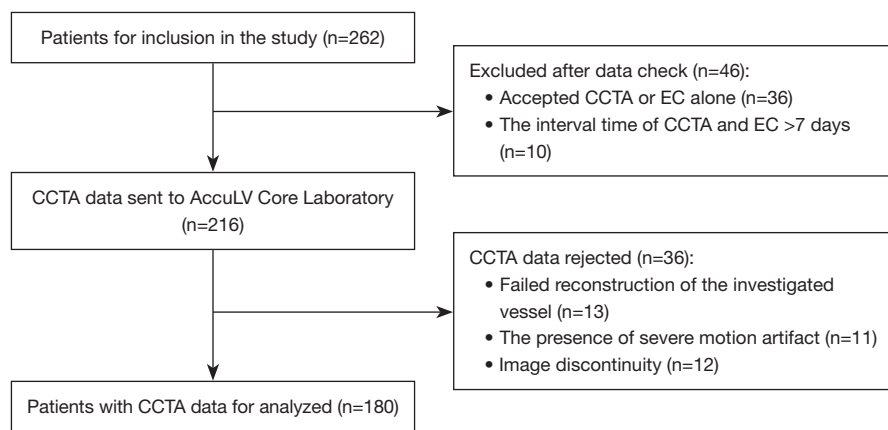


Figure 3 Participant flow chart of the study. CCTA, coronary computed tomography angiography; EC, echocardiography; AccuLV, left ventricular ejection fraction calculated by deep learning method.

Table 1 Baseline characteristics

Population characteristics	Total
Age (mean \pm SD) (years)	64.3 \pm 13.2
Males, n (%)	111 (61.7)
Previous myocardial infarction, n (%)	11 (6.1)
Previous PCI, n (%)	15 (8.3)
Hypertension, n (%)	87 (48.3)
Diabetes mellitus, n (%)	38 (21.1)
Smoking, n (%)	33 (18.3)

PCI, percutaneous coronary intervention.

Results

Patients' demographic and clinical characteristics at baseline

This study enrolled a total of 262 patients, with 46 being excluded because they received CCTA or EC alone and the interval between CCTA and EC was more than 7 days. After core laboratory analysis, 36 of the remaining 216 patients were rejected due to poor CCTA image quality: unsatisfied resolution leading to failed reconstruction of the investigated vessel (n=13), unsuccessful reconstruction due to the presence of severe motion artifact (n=11) and image discontinuity (n=12). As a result, 180 patients were included in the final analysis (Figure 3). The mean EC-LVEF and DL-LVEF values were 64.0% (52.3%, 69.0%) and 73.0% (52.3%, 77.0%), respectively. The average age was 64 \pm 13 years old. The subjects were mostly men (61.7%),

with 21.1% having type 2 diabetes mellitus (T2DM) and 48.3% having hypertension. Table 1 displays the baseline characteristics.

Correlation and agreement between EC-LVEF and DL-LVEF

Figures 4,5 show the correlation and agreement between EC-LVEF and DL-LVEF. EC-LVEF had a strong positive correlation with DL-LVEF in the overall population ($r=0.82$, $P<0.001$). The Bland-Altman analysis revealed that the DL method was highly consistent with the EC method (mean difference 0.01; 95% CI: -0.28 to 0.30).

To further compare the diagnostic efficacy of the DL algorithm in different populations, patients were divided into three groups: (I) hypertensive patients, (II) postmenopausal women, and (III) T2DM patients. EC-LVEF and DL-LVEF were found to be positively correlated for hypertensive patients ($r=0.77$, $P<0.001$), postmenopausal women ($r=0.92$, $P<0.001$) and diabetes ($r=0.88$, $P<0.001$). DL-LVEF had good agreement with EC-LVEF (mean difference 0.02; 95% CI: -0.28 to 0.32) in group I (n=87) and group II (n=23), the agreement between EC-LVEF and DL-LVEF was good (mean difference 0.02; 95% CI: -0.18 to 0.23). The mean difference between EC-LVEF and DL-LVEF in group III (n=38) was -0.01 (95% CI: -0.29 to 0.27).

Diagnostic performance of AccuLV software for predicting EC-LVEF <50%

Figure 6 depicts the discriminant function of DL method

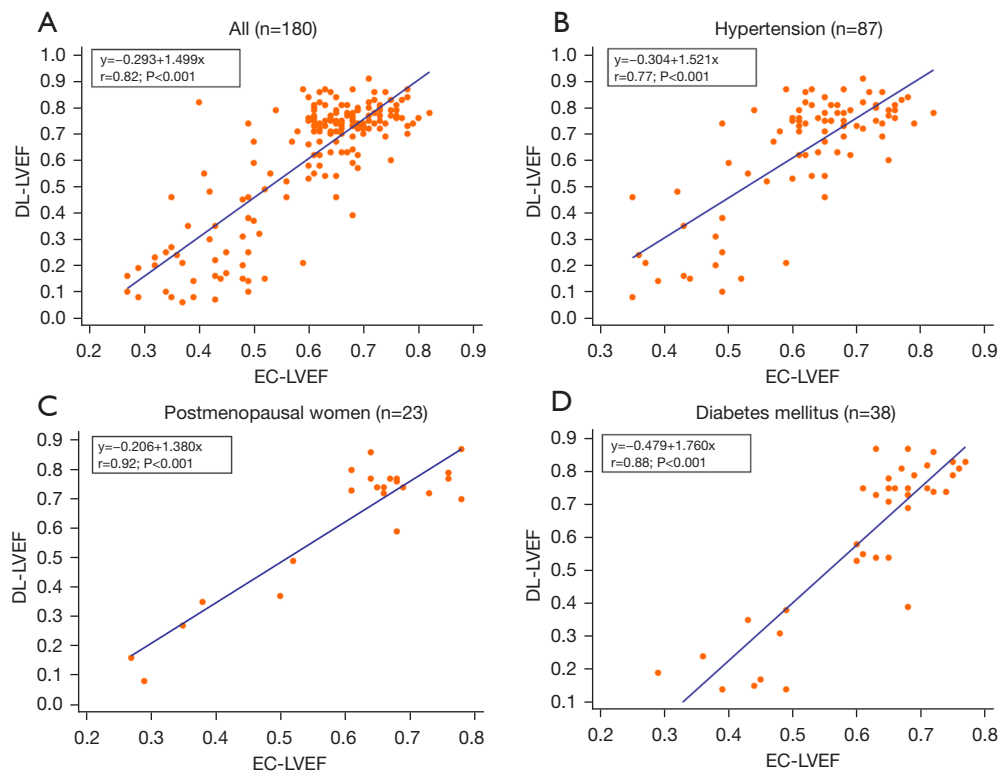


Figure 4 Linear regression plot shows the correlation between LVEF measured by DL and two-dimensional EC. (A) All patients, (B) 87 patients with hypertension, (C) 23 postmenopausal women, and (D) 38 patients with type 2 diabetes mellitus. LVEF, left ventricular ejection fraction; DL, deep learning; EC, echocardiography.

for predicting EC-LVEF $< 50\%$. The AUC value of DL method for EC-LVEF $< 50\%$ were 0.951 (95% CI: 0.901–1.000). The sensitivity, specificity, PPV, NPV, and diagnostic accuracy of DL method were 92.3%, 94.3%, 92.3%, 94.3%, and 93.9%, respectively, using EC-LVEF $< 50\%$ as a reference. The sensitivity, specificity, and diagnostic accuracy of DL method in the three subgroups are shown in *Figure 7*.

Discussion

This study aimed to assess the accuracy of a newly developed, fully automated DL algorithm for quantifying LVEF. The automated measurements were compared to EC reference values. The main findings of this study can be summarized as follows: (I) EC-LVEF and DL-LVEF were well correlated in the overall population, indicating the reliability of the DL algorithm; (II) based on the reference standard of EC-LVEF $< 50\%$, DL-LVEF exhibited excellent

diagnostic performance and could effectively evaluate LV function.

EC is a common medical image, which is mainly used to observe the real-time movement of the heart and evaluate the functional parameters of the heart, as well as to prevent and diagnose diseases. CCTA, which is also non-invasive, is a reliable substitute for cardiac MR due to its main advantages of shorter exam time (14) and lower cost (15). CCTA has become an important clinical diagnostic method for CVD (16). However, LV segmentation faces significant challenges. The LV can vary greatly in shape, size, and contrast (17). For some patients, the external wall of the LV has low contrast variations between the LV and the background, thus it is difficult to be recognized. Manual LV segmentation is a time-consuming and laborious task, and is highly susceptible to intra-observer and inter-observer variability, which increases the rate of misdiagnosis. Furthermore, most LV segmentation studies model smooth surfaces without considering the details of the heart interior.

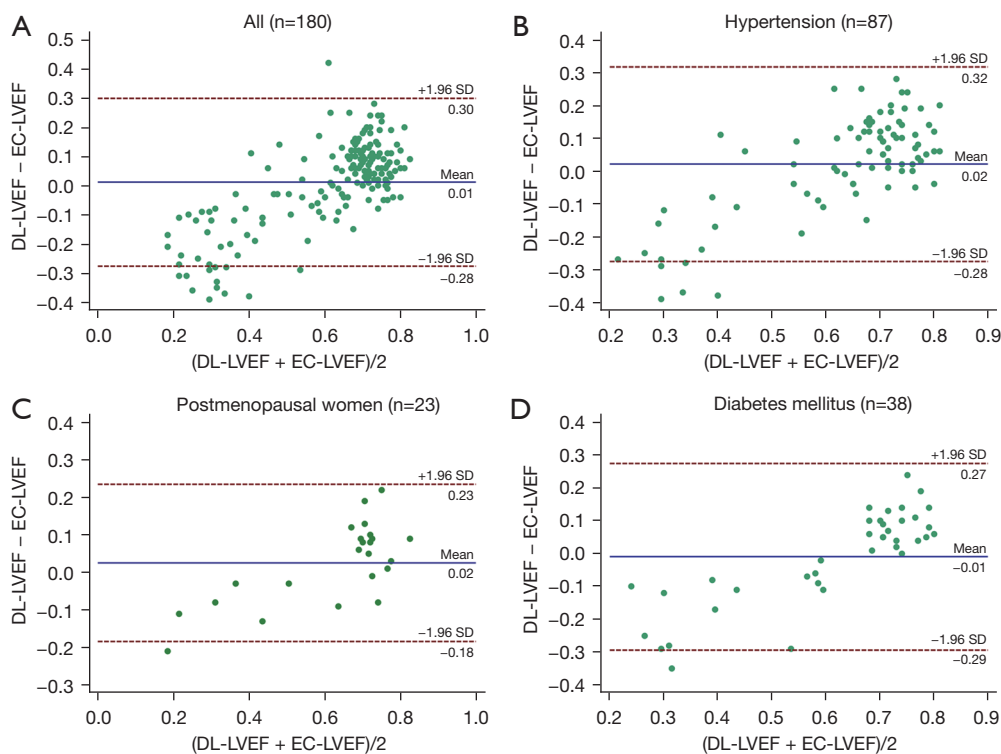


Figure 5 Bland-Altman plot for LVEF. Comparisons of EC-LVEF with DL-LVEF. (A) All patients, 6.1% patients had inconsistent measures (11/180); (B) 87 patients with hypertension, 4.6% patients (n=4) had inconsistent measures; (C) 23 postmenopausal women, 2.6% patients (n=1) had inconsistent measures; and (D) 38 patients with type 2 diabetes mellitus, 2.6% patients (n=1) had inconsistent measures. LVEF, left ventricular ejection fraction; EC, echocardiography; DL, deep learning.

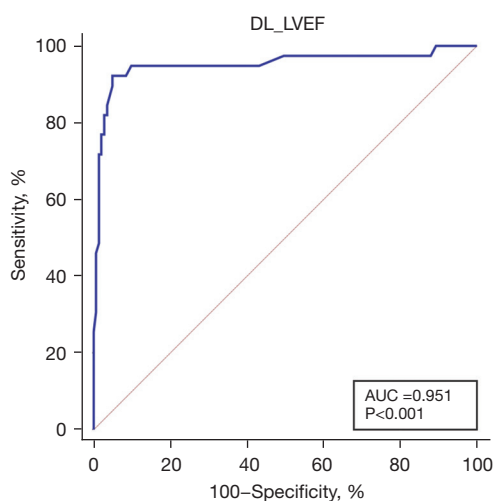


Figure 6 Overall diagnostic accuracy (area under the curve in receiver operating characteristic analysis) of DL method for detecting EC-LVEF <50% in all patients. DL, deep learning; AUC, area under the curve; EC, echocardiography; LVEF, left ventricular ejection fraction.

In this study, we proposed and evaluated a DL method based on an 8-layer residual U-Net with deep supervision for segmentation of the LV in CCTA scans. The anatomic and functional features of coronary arteries can be obtained at the same time when CCTA image data are acquired, so as to realize the non-invasive and rapid fusion of anatomy and function. Our DL approach overcomes the shortcomings of many existing methods for segmenting the LV: (I) the graph cut method is employed for image labeling, resulting in more accurate LV labeling; (II) the DL approach deepens from the original 4 to 8 layers, extracting deeper abstract information and introducing an auxiliary path for deep supervision, allowing the deep feature map loss to be obtained, enhancing model segmentation accuracy, and increasing the network fitting ability, thereby significantly improving LV recognition capacity; (III) compared to manual segmentation data analysis, the DL method exhibits higher sensitivity, specificity, and similarity; (IV) the operation is straightforward, only requiring the

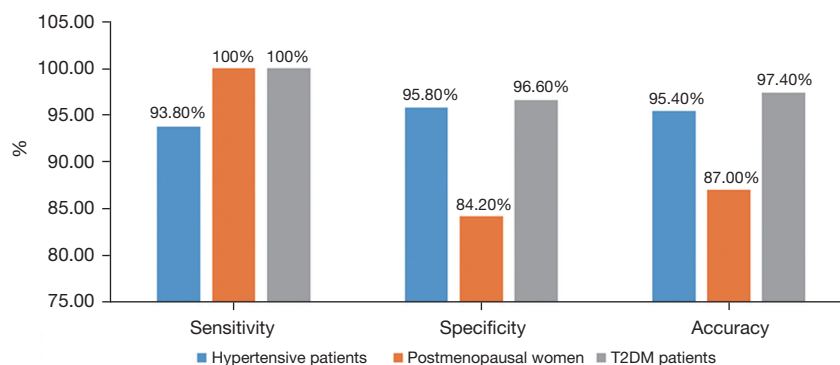


Figure 7 Comparison of DL-LVEF concordance diagnostic in three subgroups. T2DM, type 2 diabetes mellitus; DL, deep learning; LVEF, left ventricular ejection fraction.

import of standard CCTA images without the need to extract long- and short-axis sections; (V) due to the high degree of automation of AI, calculating a LVEF value takes approximately 28 s (18); (VI) it can automatically identify papillary muscles and other cardiac tissues, rendering the calculation results more reliable. The entire process is repeatable and does not necessitate human intervention.

Our findings show that the proposed 8-layer residual U-Net method is effective at delineating LV with high precision. Compared with EC, the accuracy, specificity, and sensitivity of our DL method were 93.9%, 97.8%, and 81.8%, respectively. Diabetes and hypertension are well-known cardiovascular risk factors. A higher proportion of patients with LV dysfunction have co-existing hypertension or diabetes (19,20). Reduced endogenous estrogen and progesterone levels in postmenopausal women may result in decreased LV systolic and diastolic function (21). Therefore, early quantification of LV function in these three groups is critical. To further assess the accuracy of our methods, we carried out a sub-analysis by dividing our patients into three groups: (I) hypertensive patients, (II) postmenopausal women, and (III) T2DM patients. In these three subgroups, DL-LVEF showed a good correlation and consistency with EC-LVEF. It is proven that our approach can depict LV volumes from these CCTA images effectively and accurately. The combination of deep supervision and U-Net with deeper layers improves LV segmentation performance and AccuLV may be a promising, fully automated tool for rapid and accurate quantification of LV function.

DL plays an increasingly important role in the field of medical imaging. How to use the advantage of DL to fully automate the evaluation of cardiac function has become

an important research direction in academia. Automatic evaluation of cardiac function by DL algorithm can not only greatly reduce the work burden of ultrasound doctors, but also avoid the errors of cardiac parameters caused by operator subjectivity to a certain extent. At present, DL has been widely used in the field of LV segmentation. Tromp *et al.* showed that the accuracy of DL algorithm is similar to that of manual measurement by professional sonographers, and highlight the possibility of DL to provide a fully automated solution for interpreting echocardiograms, which can support clinicians and augment clinical care (22). He *et al.* designed a blinded, randomized non-inferiority clinical trial of AI versus sonographer initial assessment of LVEF to evaluate the impact of AI in the interpretation workflow. They found that an AI-guided workflow for the initial assessment of cardiac function in EC was non-inferior and even superior to the initial assessment by the sonographer (23). The above studies and our study prove that DL has great clinical potential in the application of LV segmentation.

Limitations

There are some limitations to this study. First, the reference standard in our study was EC, which is most commonly used in clinical practice. We found inconsistencies between the DL method and the biplanar method in the diagnosis of LV insufficiency. The measurement of LVEF is influenced by many factors, such as LV remodeling. The EC biplane method relies on geometric assumptions. Geometric anomalies in the LV may also play a role in the inconsistencies between the two patterns. In addition,

echocardiograms have been reported to underestimate the volume of the LV, which is highly influenced by the operator and less reproducible. Therefore, there may be inconsistencies between the two. Second, because this is a retrospective study, it is difficult to generalize the findings. To further evaluate the diagnostic effect of DL algorithm, a large-scale prospective trial is required. Third, because follow-up data were not analyzed, we were unable to assess the prognostic implications of DL-guided treatment. DL algorithm should be studied further in the future with major adverse cardiac events (defined as the composite of all-cause death, nonfatal myocardial infarction, or unplanned revascularization at 1 year) as the primary endpoint. Fourth, the number of patients is low, in particular the number of patients with reduced LVEF, therefore, more prospective large-sample trials are needed to adequately verify the diagnostic performance of DL-LVEF.

Conclusions

The AccuLV software is founded on an innovative 8-layer residual U-Net technique incorporating deep supervision, which efficiently quantifies LV function and delivers strong diagnostic performance. Relying on CCTA images, it has the potential to serve as a safe, effective, and reliable instrument for evaluating LV function. The algorithm will undergo continuous updates in the future, and numerous multicenter prospective clinical trials will be carried out to confirm the dependability of clinical outcomes and to benefit a greater number of patients.

Acknowledgments

Funding: The present study was supported by the Major Medical and Health Science and Technology Plan of Zhejiang Province (No. WKJ-ZJ-1913), the Natural Science Foundation of Zhejiang Province (No. LY21H020002), and CCA-China Youth Clinical Research Fund (No. 2017-CCA-VG-024). The funders had no role in study design, data collection and analysis, decision to publish, or preparation of the manuscript.

Footnote

Reporting Checklist: The authors have completed the STARD reporting checklist. Available at <https://qims.amegroups.com/article/view/10.21037/qims-22-976/rc>

Conflicts of Interest: All authors have completed the ICMJE uniform disclosure form (available at <https://qims.amegroups.com/article/view/10.21037/qims-22-976/coif>). Yumeng Hu, Xiaochang Leng and Jianping Xiang are employed at ArteryFlow Technology Co., Ltd., whose products or services may be related to the subject matter of the article, although these authors provided technical support only. The other authors have no conflicts of interest to declare.

Ethical Statement: The authors are accountable for all aspects of the work in ensuring that questions related to the accuracy or integrity of any part of the work are appropriately investigated and resolved. This study was approved by the Ethics Committee of Zhejiang Hospital and conducted according to the principles of the Declaration of Helsinki (as revised in 2013). Since this clinical study was a retrospective analysis of the information of previous cases, without direct contact with the subjects and subject privacy protection, the risk borne by the subjects was not greater than the minimum risk. The Ethics Committee of Zhejiang Hospital agreed to exempt informed consent after review.

Open Access Statement: This is an Open Access article distributed in accordance with the Creative Commons Attribution-NonCommercial-NoDerivs 4.0 International License (CC BY-NC-ND 4.0), which permits the non-commercial replication and distribution of the article with the strict proviso that no changes or edits are made and the original work is properly cited (including links to both the formal publication through the relevant DOI and the license). See: <https://creativecommons.org/licenses/by-nc-nd/4.0/>.

References

1. Hartley A, Marshall DC, Saliccioli JD, Sikkil MB, Maruthappu M, Shalhoub J. Trends in Mortality From Ischemic Heart Disease and Cerebrovascular Disease in Europe: 1980 to 2009. *Circulation* 2016;133:1916-26.
2. Bui AL, Horwich TB, Fonarow GC. Epidemiology and risk profile of heart failure. *Nat Rev Cardiol* 2011;8:30-41.
3. Burns RJ, Gibbons RJ, Yi Q, Roberts RS, Miller TD, Schaer GL, Anderson JL, Yusuf S; CORE Study Investigators. The relationships of left ventricular ejection fraction, end-systolic volume index and infarct size to six-month mortality after hospital discharge following

- myocardial infarction treated by thrombolysis. *J Am Coll Cardiol* 2002;39:30-6.
4. Dahl JS, Eleid MF, Michelena HI, Scott CG, Suri RM, Schaff HV, Pellikka PA. Effect of left ventricular ejection fraction on postoperative outcome in patients with severe aortic stenosis undergoing aortic valve replacement. *Circ Cardiovasc Imaging* 2015;8:e002917.
 5. Gandotra C, Clark J, Liu Q, Senatore FF, Rose M, Zhang J, Stockbridge NL. Heart Failure Population with Therapeutic Response to Sacubitril/Valsartan, Spironolactone and Candesartan: FDA Perspective. *Ther Innov Regul Sci* 2022;56:4-7.
 6. Gevaert AB, Kataria R, Zannad F, Sauer AJ, Damman K, Sharma K, Shah SJ, Van Spall HGC. Heart failure with preserved ejection fraction: recent concepts in diagnosis, mechanisms and management. *Heart* 2022;108:1342-50.
 7. Deo SV, Sundaram V, Sahadevan J, Selvaganesan P, Mohan SM, Rubelowsky J, Josephson R, Elgudin Y, Kilic A, Cmolik B. Outcomes of coronary artery bypass grafting in patients with heart failure with a midrange ejection fraction. *J Thorac Cardiovasc Surg* 2023;165:149-58.e4.
 8. An SM, Nam JS, Kim HJ, Bae HJ, Chin JH, Lee EH, Choi IC. Postoperative changes in left ventricular systolic function after combined mitral and aortic valve replacement in patients with rheumatic heart disease. *J Card Surg* 2021;36:3654-61.
 9. Lang RM, Badano LP, Mor-Avi V, Afilalo J, Armstrong A, Ernande L, Flachskampf FA, Foster E, Goldstein SA, Kuznetsova T, Lancellotti P, Muraru D, Picard MH, Rietzschel ER, Rudski L, Spencer KT, Tsang W, Voigt JU. Recommendations for cardiac chamber quantification by echocardiography in adults: an update from the American Society of Echocardiography and the European Association of Cardiovascular Imaging. *Eur Heart J Cardiovasc Imaging* 2015;16:233-70.
 10. Kusunose K, Abe T, Haga A, Fukuda D, Yamada H, Harada M, Sata M. A Deep Learning Approach for Assessment of Regional Wall Motion Abnormality From Echocardiographic Images. *JACC Cardiovasc Imaging* 2020;13:374-81.
 11. Ronneberger O, Fischer P, Brox T. U-Net: Convolutional Networks for Biomedical Image Segmentation. *International Conference on Medical Image Computing & Computer-assisted Intervention* 2015:234-41.
 12. Dou Q, Yu L, Chen H, Jin Y, Yang X, Qin J, Heng PA. 3D deeply supervised network for automated segmentation of volumetric medical images. *Med Image Anal* 2017;41:40-54.
 13. Chow BJ, Wells GA, Chen L, Yam Y, Galiwango P, Abraham A, Sheth T, Dennie C, Beanlands RS, Ruddy TD. Prognostic value of 64-slice cardiac computed tomography severity of coronary artery disease, coronary atherosclerosis, and left ventricular ejection fraction. *J Am Coll Cardiol* 2010;55:1017-28.
 14. Fu H, Wang X, Diao K, Huang S, Liu H, Gao Y, Zhao Q, Yang ZG, Guo YK. Correction to: CT compared to MRI for functional evaluation of the right ventricle: a systematic review and meta-analysis. *Eur Radiol* 2020;30:4705-8.
 15. Centonze M, Lorenzin G, Francesconi A, Cademartiri F, Casagrande G, Fusaro M, Ligabue G, Zanetti G, Spanti D, De Cobelli F. Cardiac-CT and Cardiac-MR examinations cost analysis, based on data of four Italian Centers. *Radiol Med* 2016;121:12-8.
 16. Techasith T, Cury RC. Stress myocardial CT perfusion: an update and future perspective. *JACC Cardiovasc Imaging* 2011;4:905-16.
 17. Medina R, Bautista S, Vanegas P, Morocho V. Left ventricle myocardium segmentation in multi-slice computerized tomography, Andescon 2017. doi: 10.1109/ANDESCON.2016.7836246.
 18. Li C, Song X, Zhao H, Feng L, Hu T, Zhang Y, Jiang J, Wang J, Xiang J, Sun Y. An 8-layer residual U-Net with deep supervision for segmentation of the left ventricle in cardiac CT angiography. *Comput Methods Programs Biomed* 2021;200:105876.
 19. Jiang L, Wang J, Liu X, Li ZL, Xia CC, Xie LJ, Gao Y, Shen MT, Han PL, Guo YK, Yang ZG. The combined effects of cardiac geometry, microcirculation, and tissue characteristics on cardiac systolic and diastolic function in subclinical diabetes mellitus-related cardiomyopathy. *Int J Cardiol* 2020;320:112-8.
 20. Roger VL, Go AS, Lloyd-Jones DM, Adams RJ, Berry JD, Brown TM, et al. Heart disease and stroke statistics--2011 update: a report from the American Heart Association. *Circulation* 2011;123:e18-e209.
 21. Harlow SD, Gass M, Hall JE, Lobo R, Maki P, Rebar RW, Sherman S, Sluss PM, de Villiers TJ; . Executive summary of the Stages of Reproductive Aging Workshop + 10: addressing the unfinished agenda of staging reproductive aging. *Fertil Steril* 2012;97:843-51.
 22. Tromp J, Seekings PJ, Hung CL, Iversen MB, Frost MJ, Ouwerkerk W, Jiang Z, Eisenhaber F, Goh RSM, Zhao H, Huang W, Ling LH, Sim D, Cozzone P, Richards

- AM, Lee HK, Solomon SD, Lam CSP, Ezekowitz JA. Automated interpretation of systolic and diastolic function on the echocardiogram: a multicohort study. *Lancet Digit Health* 2022;4:e46-e54.
23. He B, Kwan AC, Cho JH, Yuan N, Pollick C, Shiota T,

Ebinger J, Bello NA, Wei J, Josan K, Duffy G, Jujjavarapu M, Siegel R, Cheng S, Zou JY, Ouyang D. Blinded, randomized trial of sonographer versus AI cardiac function assessment. *Nature* 2023;616:520-4.

Cite this article as: Zhang J, Yang L, Hu Y, Leng X, Huang W, Liu Y, Liu X, Wang L, Zhang J, Li D, Tang L, Xiang J, Du C. Calculation of left ventricular ejection fraction using an 8-layer residual U-Net with deep supervision based on cardiac CT angiography images versus echocardiography: a comparative study. *Quant Imaging Med Surg* 2023;13(9):5852-5862. doi: 10.21037/qims-22-976